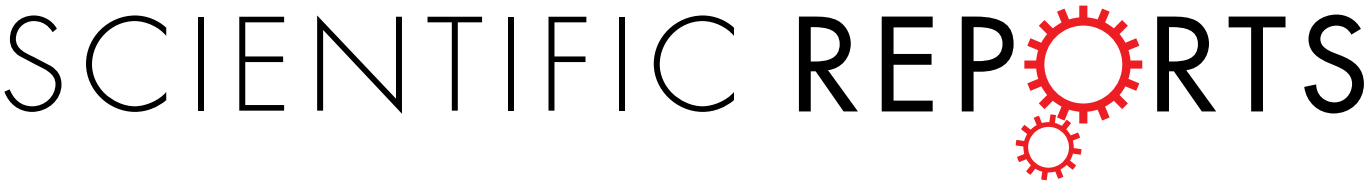

OPEN

Received: 9 March 2017
Accepted: 29 January 2018
Published online: 12 February 2018

Carbonate chemistry of an in-situ free-ocean CO_2 enrichment experiment (antFOCE) in comparison to short term variation in Antarctic coastal waters

J. S. Stark[1], N. P. Roden[1,2], G. J. Johnstone[1], M. Milnes[1], J. G. Black[2], S. Whiteside[1], W. Kirkwood[3], K. Newbery[1], S. Stark[1], E. van Ooijen[4,5], B. Tilbrook[4,5], E. T. Peltzer[3], K. Berry[4,5] & D. Roberts[5]

Free-ocean CO_2 enrichment (FOCE) experiments have been deployed in marine ecosystems to manipulate carbonate system conditions to those predicted in future oceans. We investigated whether the pH/carbonate chemistry of extremely cold polar waters can be manipulated in an ecologically relevant way, to represent conditions under future atmospheric CO_2 levels, in an *in-situ* FOCE experiment in Antarctica. We examined spatial and temporal variation in local ambient carbonate chemistry at hourly intervals at two sites between December and February and compared these with experimental conditions. We successfully maintained a mean pH offset in acidified benthic chambers of −0.38 (±0.07) from ambient for approximately 8 weeks. Local diel and seasonal fluctuations in ambient pH were duplicated in the FOCE system. Large temporal variability in acidified chambers resulted from system stoppages. The mean pH, Ω_{arag} and fCO_2 values in the acidified chambers were 7.688 ± 0.079, 0.62 ± 0.13 and 912 ± 150 µatm, respectively. Variation in ambient pH appeared to be mainly driven by salinity and biological production and ranged from 8.019 to 8.192 with significant spatio-temporal variation. This experiment demonstrates the utility of FOCE systems to create conditions expected in future oceans that represent ecologically relevant variation, even under polar conditions.

The level of anthropogenic carbon dioxide (CO_2) in the atmosphere continues to rise in line with the highest Intergovernmental Panel on Climate Change (IPCC) emissions scenario, representative concentration pathway (RCP) 8.5[1–3]. The oceans have absorbed approximately 28% of CO_2 emitted since 1850[4]. This increase in oceanic CO_2 causes an increase in the hydrogen ion concentration [H^+] and has resulted in a decrease in seawater pH of 0.1[5] and an accompanying decrease in the saturation state (Ω) of calcium carbonate ($CaCO_3$). This process – known as ocean acidification – causes significant changes in the chemistry of seawater, particularly the carbonate system. Under IPCC emission scenarios for increasing CO_2, ocean pH is predicted to decline by a further 0.2 to 0.4 by 2100[6]. This may have serious consequences for marine ecosystems[5], from direct effects on physiology, metabolism, and availability of carbonate to build shells and skeletons for many species; to indirect effects on food webs and species interactions[7].

Polar waters have naturally low carbonate ion concentrations, making them particularly susceptible to ocean acidification, due to a higher CO_2 solubility in cold water, sensitivity of acid-base disassociation coefficients, and oceanic circulation[8,9]. The Southern Ocean is predicted to be one of the first regions to experience widespread

[1]Antarctic Conservation and Management Theme, Australian Antarctic Division, 203 Channel Hwy, Kingston, 7050, Tasmania, Australia. [2]Institute for Marine and Antarctic Studies, University of Tasmania, 20 Castray Esplanade, Hobart, Australia. [3]Monterey Bay Aquarium Research Institute, 7700 Sandholdt Rd, Moss Landing, CA, 95039, United States of America. [4]CSIRO Oceans and Atmosphere, Castray Esplanade, Hobart, TAS 7000, Australia. [5]Antarctic Climate and Ecosystems Cooperative Research Centre, University of Tasmania, 20 Castray Esplanade, Hobart, Tasmania, 7000, Australia. J. S. Stark and N. P. Roden contributed equally to this work. Correspondence and requests for materials should be addressed to J.S.S. (email: jonny.stark@aad.gov.au)

undersaturation of aragonite, a major biogenic form of $CaCO_3$, by 2050[5] or as early as 2030 when seasonal variation of carbonate chemistry is considered[10]. Undersaturation in Arctic seas could occur as early as 2020[11]. Dissolution of aragonitic shells has already been observed in pelagic pteropods in the Southern Ocean[12]. These changes may have serious consequences for many calcifying organisms in polar regions and alter the structure and biodiversity of polar ecosystems at multiple trophic levels[5,13]. There is currently a relative paucity of knowledge of the effects of ocean acidification on polar marine organisms and ecosystems in comparison to other latitudes[8]. There are also relatively few high resolution or long-term observations of natural spatial or temporal variation of carbonate chemistry in Antarctic waters.

Free-ocean CO_2 enrichment (FOCE) systems were developed to address the need for *in-situ* studies of the effects of ocean acidification over long time scales[14]. Other *in-situ* methods for investigating ocean acidification, such as natural analogue CO_2 vents, are complicated by factors outside of the experimenters' control such as regulation of treatment conditions, selection of reference sites, large temporal variability[15], uncontrolled environmental changes and migration of organisms into and out of the study areas[14]. FOCE systems allow for the precise control of pH (by CO_2 enrichment) as an offset from ambient pH, whilst allowing for natural variation in other environmental parameters; and for long term experiments (from weeks to months) on intact communities, including examination of indirect effects such as species interactions and food webs[14]. They provide a crucial link between organism level studies and scaling up to ecosystem effects[16,17].

Carbonate chemistry of coastal systems can be highly variable on timescales from days to months, with multiple drivers including freshwater input, primary productivity and seasonal upwelling[18,19]. The interaction between biological and geochemical processes in coastal ecosystems has the potential to either exacerbate or mitigate ocean acidification effects[19]. The frequency, amplitude and duration of carbonate chemistry events that cross ecological thresholds will be crucial to understanding effects of ocean acidification on coastal organisms[19]. Future changes in Antarctic coastal carbonate chemistry will be influenced by changes in sea ice, stratification and mixing, freshwater inputs[20,21] and biological processes[18]. Observations of pH from Antarctic coastal waters are sparse and very limited, but have been shown in some areas to have variability of a similar magnitude to kelp forests and coral reefs[22–24]. There is a critical need for high resolution records of pH in Antarctic coastal waters to understand current conditions, variability, regional differences and how these areas may respond to future change.

FOCE systems were developed at the Monterey Bay Aquarium Research Institute (MBARI)[25,26] and have been deployed in various locations around the world[14]. FOCE systems consist of semi-open flow-through chambers enclosing a section of the seabed, into which a small quantity of CO_2 enriched seawater is introduced, usually via a duct or flume to allow equilibration of pH before exposure inside the chambers. The manipulation of pH is usually done as an offset[27,28] from ambient conditions, incorporating natural variation in pH in the acidified treatments. They are semi-open systems in that the primary water source comes from outside the chambers, incorporating natural variation in background physicochemical variables such as temperature, oxygen and salinity, as well as biogeochemical and biological variables such as nutrients, food and propagules. The incorporation of natural variation into the FOCE experiment is one of the most important features in creating realistic experimental 'future ocean' treatments. There have been no previous attempts to manipulate pH in polar waters using these methods, where the reaction kinetics of CO_2 in seawater are strongly influenced by low temperatures[29]. *In situ* manipulation of seawater carbonate chemistry requires sufficient periods of equilibration to stabilise experimental conditions[14,29].

Here we investigate whether it is possible in polar waters to create ecologically meaningful pH conditions predicted in future oceans using FOCE technology. We also examined the variation in pH and other parameters at a coastal Antarctic site over a 3 month period between December and February at a high temporal resolution of hourly measurements. We describe the performance of the antFOCE system and report on the changes in carbonate chemistry that were observed during the experiment, in relation to observations of ambient pH at the experimental site, O'Brien Bay, Casey Research Station, East Antarctica. We aimed to achieve a pH perturbation of −0.4 from ambient, in line with IPCC predictions under business as usual emissions scenarios for the year 2100, which equates to atmospheric CO_2 levels of approximately 936 ppm (IPCC AR4, SRES A1FI, and AR5 RCP8.5)[30]. By maintaining a pH offset of −0.4 and allowing for natural pH variation, the pH in the acidified chambers would vary according to diel, tidal, seasonal and other factors that influence pH in coastal waters.

Results

Manipulation of the carbonate system and pH. The biogeochemical parameters in the antFOCE system, measured from 19 December 2014 to 27 February 2015, are summarized in Fig. 1 and weekly averages shown in Supplementary Table S1. The antFOCE deployment period is divided into two separate phases, a two-week acclimatization phase and an eight-week experimental phase. During the acclimatization phase, the pH of the acidified chambers was gradually lowered by incrementally increasing the amount of CO_2 Enriched Seawater (ESW) introduced into the chambers until the target pH reduction of 0.4 relative to the control chambers was reached. During the eight-week experimental phase, a mean pH offset of -0.383 ± 0.066 and -0.382 ± 0.065 was achieved for chambers A and B respectively. This resulted in aragonite undersaturation, with mean Ω_{ar} values of 0.62 ± 0.15 and 0.62 ± 0.13 and mean fCO_2 values of 914 ± 159 µatm and 911 ± 150 µatm (Supplementary Table S1) in the acidified chambers. The control chambers during the experimental phase had a mean Ω_{ar} of 1.39 ± 0.11. The mean fCO_2 in the control chambers was 354 ± 42 µatm and in the ambient environment was 341 ± 25 µatm, which was undersaturated with respect to the mean atmospheric fCO_2 value of 379 ± 3 µatm (1 s.d.).

A comparison of measured Total Alkalinity (TA) values in the acidified and control chambers showed no detectable increase as a result of $CaCO_3$ dissolution (Fig. 2), despite the acidified chambers having undersaturated Ω_{ar}. This was initially determined by normalising (n) the sum of TA and nitrate (TA + N) concentrations to the mean salinity of 33.645 observed during the antFOCE deployment period. This accounts for changes in these

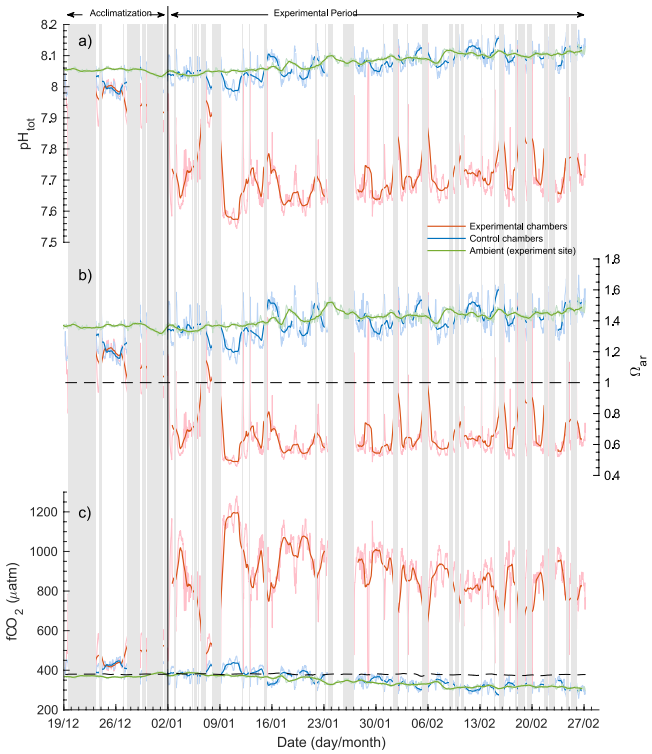

Figure 1. Carbonate chemistry conditions within the experimental chambers and in ambient seawater during the acclimatization and experimental periods of the antFOCE experiment. (**a**) Measured pH_{tot}; (**b**) calculated saturation state of aragonite (Ω_{ar}); (**c**) calculated fugacity of CO_2 (fCO_2) (µatm) of seawater with atmospheric fCO_2 shown as dashed line. Green line = ambient conditions at experiment site; red line = acidified chambers (mean of chambers A and B); blue line = control chambers (chambers C and D combined). Lighter coloured lines show high-resolution measurements (taken every 30 min), with darker coloured lines showing 24 hour low-pass (moving average) filtered data. The grey bars represent periods of experimental system downtime.

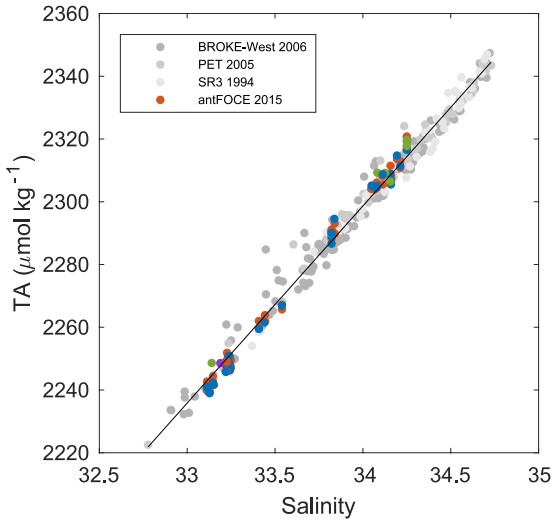

Figure 2. The salinity and TA relationship in waters south of 60°S and shallower than 500 m, including the antFOCE experiment. Grey dots show data from BROKE-West in 2006, the Princess Elizabeth Trough in 2005 (PET) and the WOCE SR3 transect in 1994 (data available from GLODAPv2). Coloured dots show values measured in this study (red = acidified chambers, blue = control chambers, green = ambient seawater at experiment site, purple = ambient seawater at outer O'Brien Bay). A linear regression yielded the following equation, $y = (62.8 \pm 0.4)x + (163 \pm 13)$ ($n = 340$, $r^2 = 0.99$, standard error = 4 µmol kg^{-1}).

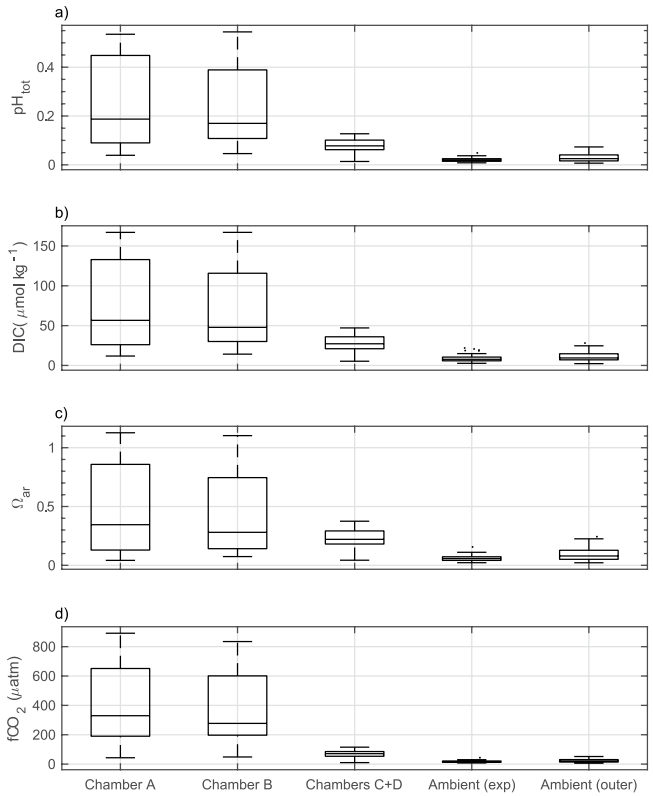

Figure 3. Summary of daily changes in seawater parameters within O'Brien Bay over the duration of the experiment. Boxes show the interquartile and median daily range. The whisker length is 1.5x the interquartile range. Dots show data points that lie outside of that range. Data shown are of (**a**) pH total scale (pH_{tot}), (**b**) calculated dissolved inorganic carbon (DIC), (**c**) saturation state of aragonite (Ω_{ar}) and (**d**) fugacity of CO_2 (fCO_2). Chambers A and B are the acidified chambers; chambers C+D are the combined values of the control chambers; Ambient (exp) shows the natural conditions at the site of the experiment; Ambient (outer) shows conditions at the outer site in O'Brien Bay.

parameters as a result of freshwater input/removal, and summing the concentrations of TA and nitrate accounts for changes in TA associated with the uptake or release of dissolved nitrate during photosynthesis or respiration[31]. Consequently, both the acidified and control chambers had similar mean $nTA + nN$ values of $2302 \pm 3\,\mu mol\,kg^{-1}$ (1 s.d.; n = 57) and $2301 \pm 3\,\mu mol\,kg^{-1}$ (1 s.d.; n = 28), respectively. This result is not unexpected given the short residence time of water within the chambers of ~67 seconds. If we assume a maximum dissolution rate[32], porosity and carbonate content within the sediments (<10%, actual values range from 1–3%), the expected flux of alkalinity due to $CaCO_3$ dissolution equates to only $0.0009\,\mu mol\,L^{-1}$, which would be undetectable given the accuracy and precision of the TA measurements of $\pm 1.3\,\mu mol\,kg^{-1}$ (see methods).

During the acclimatization and experimental phases, the system experienced a series of power outages and stoppages due to equipment failure. The failure of the onsite power generator, due to a faulty oil pressure sensor, caused the majority of these outages except for two occasions, where the failure of individual thrusters, drawing water through the chambers, resulted in system stoppages. Divers replaced the damaged thrusters and the system was restarted within 24 hours. During these system stoppages, CO_2 system parameters within the acidified chambers would slowly revert back to ambient conditions until the system could be restarted. Because measuring the pH of the chambers relied on an external power supply, we were unable to characterize the biogeochemical conditions within the chambers during these short periods. Therefore, the results we report here represent the conditions within the antFOCE chambers from when the system was fully operational. Upon restarting the experimental system the pH was gradually brought back to the desired offset from ambient. This would typically be achieved over a 2 to 4 hour period. Over the 14 day acclimatization period, 8.55 days were lost due to system stoppages, and over the 56 day experimental period, 12.19 days were lost due to system stoppages (downtime), as indicated by the grey shaded areas on Fig. 1 and summarized in Supplementary Table S1.

These system stoppages resulted in increased variability within the chambers (Fig. 3) and in particular within the acidified chambers, which had a mean pH diel variability of 0.24 ± 0.17 in comparison to a mean of 0.077 ± 0.027 in the controls and a mean of 0.020 ± 0.008 in ambient seawater at the site (Supplementary Table S2). The mean values of carbonate system parameters within the control chambers throughout the experimental period, when considered over weekly intervals, were similar to those observed in the ambient environment (Fig. 1, Supplementary Table S1).

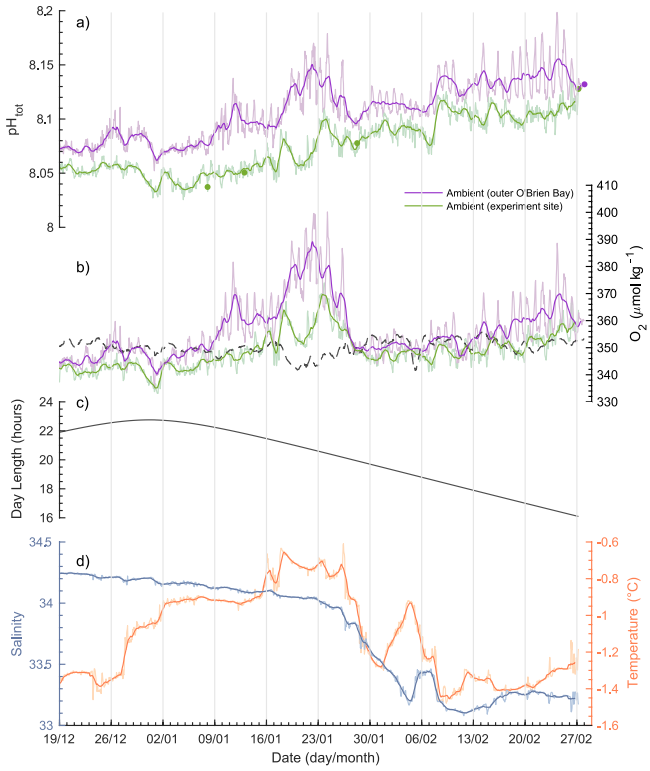

Figure 4. Ambient seawater conditions at two sites in O'Brien Bay, Casey Research Station, Antarctica, the site of the antFOCE experiment. Measurements were made between 19 December 2014 and 28 February 2015. (**a**) pH_{tot} (dots show calibration points where discrete samples were taken for analysis); (**b**) dissolved oxygen (O_2) with oxygen saturation shown as dashed line; (**c**) day length at O'Brien Bay (hours); (**d**) salinity and seawater temperature from the experiment site. Lighter coloured lines show high-resolution (hourly) measurements, with darker coloured lines showing 24-hour low-pass (moving average) filtered data.

High resolution ambient variability. There was a significant linear increase in observed ambient pH at both sites during the three month period (Experiment site $R^2 = 0.75$, $p < 0.0001$; Outer site $R^2 = 0.67$, $p < 0.0001$) with a seasonal pH range of 8.025 to 8.137 at the experimental site and 8.052 to 8.198 at the outer site (Fig. 4a, Supplementary Table S2b). Oxygen concentration at both sites peaked in late-January (Fig. 4b), just before a significant decrease in salinity was observed throughout the bay (Fig. 4d) due to an influx of glacial melt water. Temperature and salinity were very similar at both sites (Fig. 5e–h; 6e,f). Ambient pH and oxygen concentration were generally higher at the outer O'Brien Bay site than at the experiment site (Supplementary Table S2 and Figs 4 and 6).

In comparison to the experiment site (Fig. 5a), the outer site experienced an increase in short-term (diel) pH variability (Fig. 5b) over the deployment period. The range in dissolved oxygen concentrations over the duration of the experiment was also smaller at the experiment site (Figs 5c, 6d) compared to the outer site (Figs 5d, 6d). The aragonite saturation state and fCO_2 were also more variable at the outer site (Fig. 5i–l). Sea-ice cover of different thickness and age characterized these two locations, with multi-year sea ice over the experimental site measuring 260 cm in thickness, and first-year ice over the outer O'Brien Bay site measuring 150 cm in thickness at the start of the deployment.

There were significant differences in pH at both sites at all temporal scales examined: month, week, day, diel and hour (PERMANOVA analysis, Table 1). The relative magnitude of the effect size of each scale indicated that, as expected, the largest differences were between different months. Variation in pH at hourly (residual), diel, and daily intervals were of the same magnitude at the inner site, but at the outer site the diel variation had a much great effect size than daily variation (Table 1).

The dissolved oxygen concentration was, on average, 8 µmol kg^{-1} higher and the calculated DIC concentration ~13 µmol kg^{-1} lower at the outer site (Supplementary Table S2). Dividing the difference in oxygen concentration by 1.4 allows this value to be expressed in terms of organic carbon production, or DIC uptake[33,34]. Therefore, for a photosynthetic oxygen production of 8 µmol kg^{-1}, an approximate 6 µmol kg^{-1} of DIC uptake would be expected. This explains the majority of the offset observed between the two sites when the uncertainty of calculated DIC concentrations (±4 µmol kg^{-1}) is considered. However, when biological changes between the two sites are calculated over daily intervals, the outer site was not significantly different from the experimental site (Supplementary Fig. S3). This is highlighted by the mean daily values of net community production (NCP; *NCP = Net Primary Production – Heterotrophic Respiration*) of 3 ± 38 mmol C m^{-2} day^{-1} (1 s.d.; 73 days) at the experimental site (range of −68 to 131 mmol C m^{-2} day^{-1}) and 2 ± 48 mmol C m^{-2} day^{-1} (1 s.d.) at the outer site (range of −142 to 101 mmol C m^{-2} day^{-1}). Other contributors to daily changes in DIC, namely air-sea flux and ice formation and

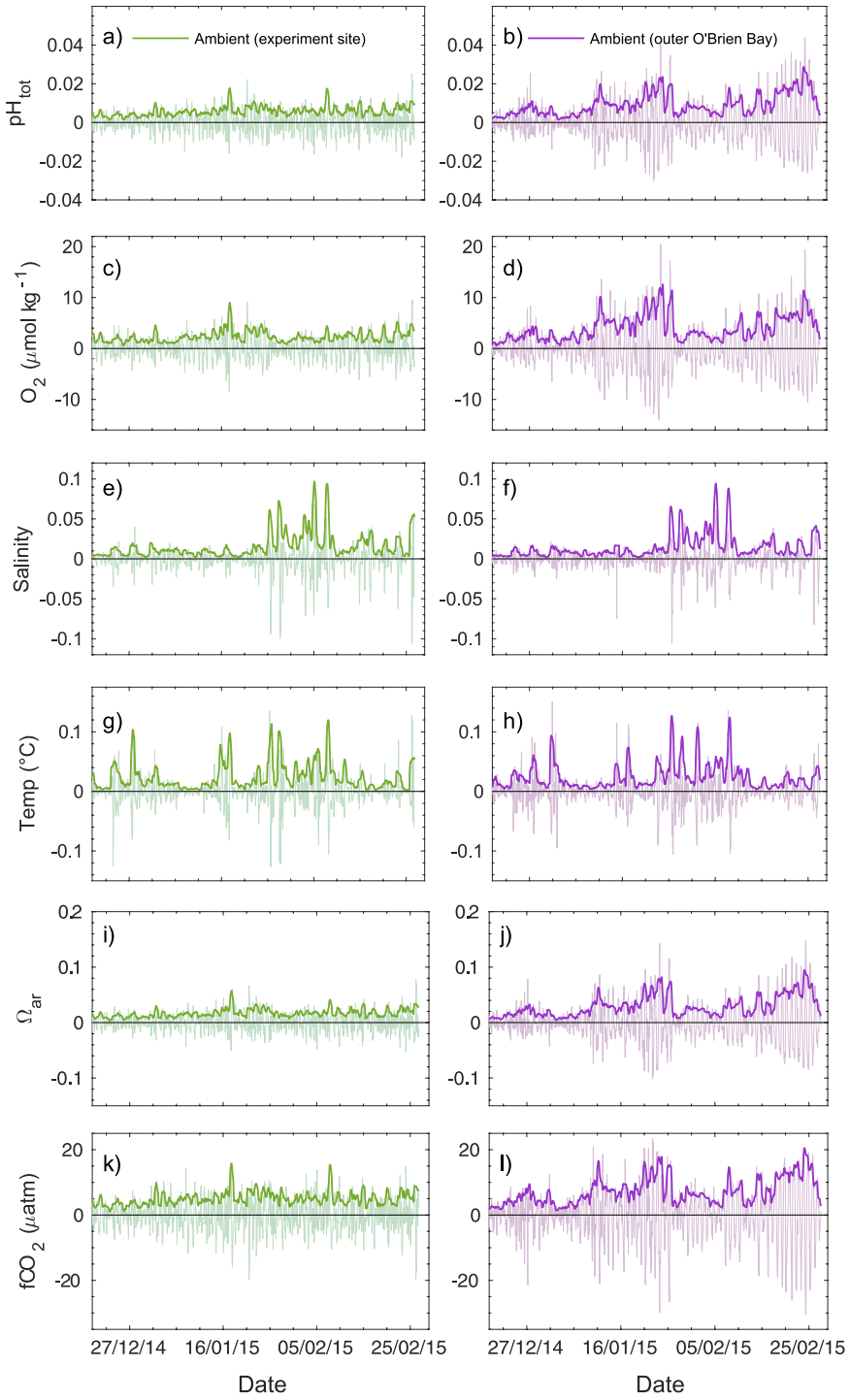

Figure 5. Short-term variability (diel changes) in ambient seawater conditions at two sites in O'Brien Bay, Casey station Antarctica. High pass filtered data showing: (**a**) and (**b**) pH_{tot}; (**c**) and (**d**) dissolved oxygen (µmol kg^{-1}); (**e**) and (**f**) salinity; (**g**) and (**h**) temperature (°C); (**i**) and (**j**) aragonite saturation state; (**k**) and (**l**) fugacity of CO_2. The zero represents a moving 24-hour average value at any given time. Darker coloured lines are the standard deviation of the 24-hour moving average of the high-frequency data (lighter coloured lines).

melt, also show similar contributions between each site (Supplementary Fig. S3). The largest changes in DIC were caused by freshwater input from ice melt, observed in late January and early February. Even though seawater fCO_2 was mostly undersaturated with respect to the atmosphere, 100% sea ice cover for the duration of the study caused the air-sea CO_2 flux to be near zero. NCP was however, extremely variable on short timescales, switching from net production to net heterotrophy from day to day (Supplementary Fig. S3).

Distance based linear modelling (DISTLM[35]), using permutation tests[36], was used to investigate correlative relationships between pH and other variables. This indicated that a significant proportion of the variation in pH

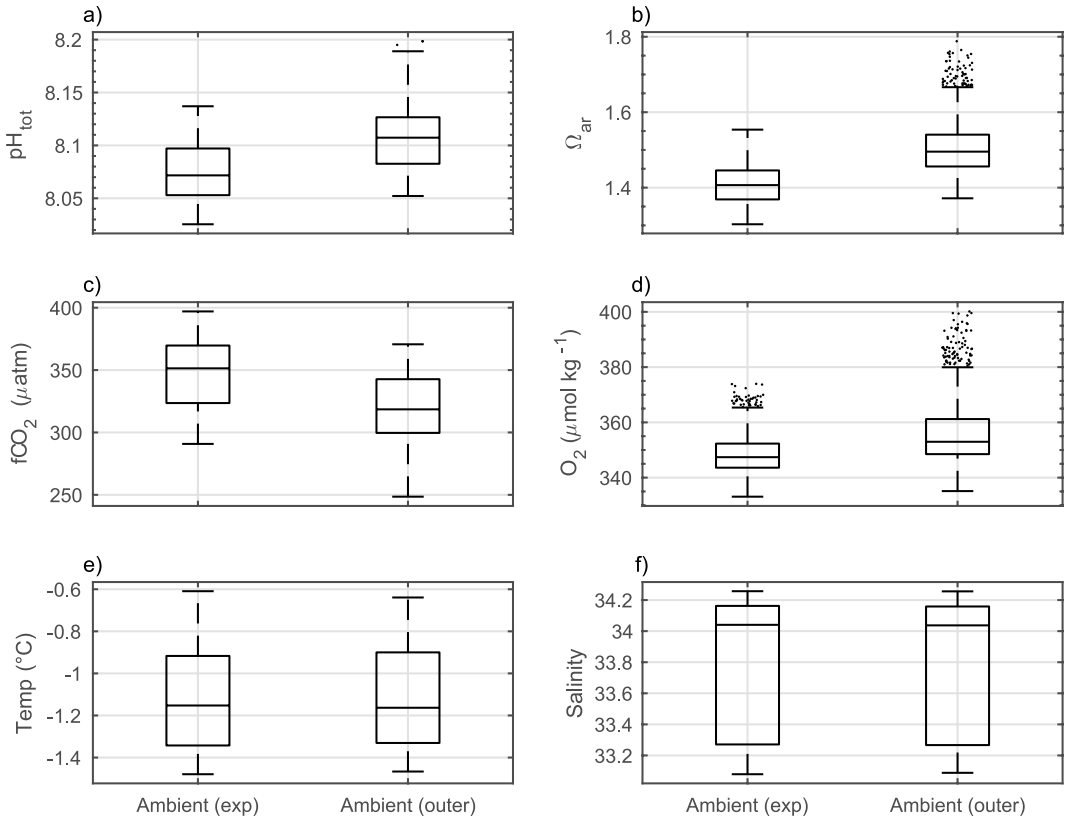

Figure 6. Summary of summer ambient seawater conditions within O'Brien Bay, the site of the antFOCE experiment between 19 December 2014 and 27 February 2015. Boxes show the interquartile range and median values. The whisker length is 1.5x the interquartile range. Dots show data points that lie outside of that range. Data shown are of (**a**) pH total scale (pH_{tot}), (**b**) saturation state of aragonite (Ω_{ar}), (**c**) fugacity of CO_2 (fCO_2), (**d**) dissolved oxygen (O_2), (**e**) temperature and (**f**) salinity. Ambient (exp) shows the natural conditions at the site of the experiment; Ambient (outer) shows conditions at the outer site in O'Brien Bay.

Experiment site						Outer site				
Source	**Df**	**MS**	**Pseudo-F**	**P**	**% var**	**Df**	**MS**	**Pseudo -F**	**P**	**% var**
Month	2	0.319	13.4	0.001	70	2	0.290	9.2	0.002	54
Week (Month)	9	0.028	33.6	0.001	22	9	0.036	14.2	0.001	24
Day (Wk(Mth))	62	0.0008	2.9	0.001	3	62	0.003	2.1	0.003	6
Diel (D(W(M)))	73	0.0003	11.1	0.001	3	74	0.001	20.7	0.001	10
Hour (Residual)	1605	0.00003			3	1622	0.00006			6
Total	1751					1769				

Table 1. PERMANOVA table of results for temporal differences in pH at nested hierarchical scales. % var = Estimates of components of variation of pH at each temporal scale.

Experiment site					Outer site			
Marginal test								
Variable	**SS (trace)**	**Pseudo-F**	**P**	**Prop.**	**SS (trace)**	**Pseudo-F**	**P**	**Prop.**
Oxygen	0.41	1019.5	0.001	0.37	0.63	1574.4	0.001	0.47
Temperature	0.19	365.48	0.001	0.17	0.02	27.607	0.001	0.02
Salinity	0.88	6973.3	0.001	0.80	0.71	1991.3	0.001	0.53
	R^2	RSS			R^2	RSS		
Combined model	0.96	0.040			0.95	0.064		

Table 2. Results of distance based linear modelling (DistLM) analysis of pH using salinity, temperature and oxygen concentration as predictor variables. Prop. = proportion of variance explained; RSS = residual sums of squares. Combined model includes all three variables.

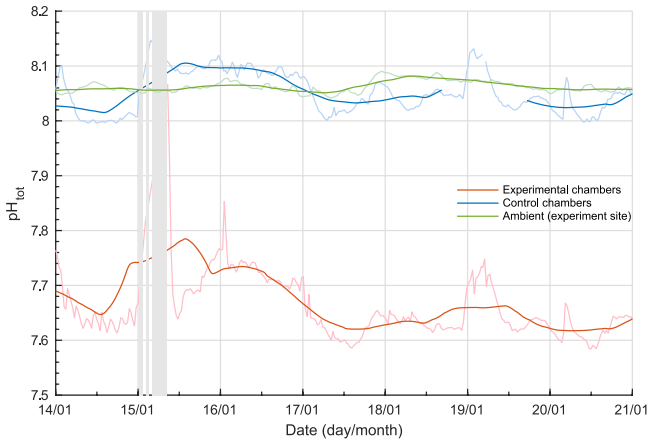

Figure 7. High-resolution record of pH in the antFOCE experiment and in the ambient seawater over a 7-day period. Measurements of pH_{tot} taken between 14 January 2015 and 21 January 2015. Green line = ambient pH at experiment site; red line = pH of acidified chambers (mean of chambers A and B); blue line = pH of control chambers (chambers C and D combined). Lighter coloured lines show high-resolution measurements, with darker coloured lines showing 24-hour low-pass (moving average) filtered data. The grey bars represent periods of experimental system downtime.

in models could be explained individually by either salinity, oxygen or temperature, but the amount of variation explained differed between the experiment site and the outer site (Table 2). Salinity could account for 80% of the variation in pH at the experiment site, followed by oxygen (37%). Salinity and oxygen explained similar levels of variation in pH at the outer site, but temperature had only a very weak relationship with pH (Table 2). Oxygen accounted for a much higher percentage of pH variation at the outer site than the experiment site, corresponding to greater variation in oxygen (Fig. 5c,d) and NCP (Supplementary Fig. S3) at the outer site. Linear models containing all three variables (salinity, oxygen and temperature) explained approximately 95% of the variation in pH at both sites (Table 2).

Discussion

Unlike free-air CO_2 experiments (FACE)[37] where simple CO_2 addition to the air is all that is required, the reaction of CO_2 with water in seawater introduces a kinetic delay that is both time and temperature dependent[29]. Given the very slow kinetics in very cold Antarctic waters, in order to be completely free and open, a FOCE experiment would need a ring of CO_2 emitters that would be eminently impractical both in size and CO_2 requirements to ensure that a sufficiently large portion of the "enclosure" would experience equilibrium of the CO_2 enrichment at maximum seawater velocities for the region. The flume design used in FOCE is thus a compromise between the ideal fully open system and one where the CO_2 conditions are within the experimenters' control. The antFOCE system successfully altered the *in-situ* carbonate chemistry in acidified chambers to conditions predicted in future oceans, maintaining a pH offset of −0.38 (±0.07). Conditions in control chambers closely matched background ambient fluctuations, but variation in acidified chambers was greater than that observed in the local ambient environment. There was considerable natural diel variation, however, towards the end of the deployment period in late February. The antFOCE system experienced several technical challenges including thruster (flow regulator) failure and problems with maintaining a reliable power supply in a remote location, which altered the experimental manipulation of carbonate conditions. Power outages were attributed, post-experiment, to a faulty oil pressure sensor in the power generator, and were the main technical issue experienced during the experiment. These problems could largely be avoided in future FOCE designs through the implementation of backup power systems. Aspects of the system that worked well included the surface housed sensor system, making water sampling and maintenance of sensors convenient and straightforward. The Honeywell Durafet pH sensors proved to be highly reliable in monitoring pH in both the experimental system and in the ambient environment.

Manipulation of carbonate chemistry in relation to natural variation. Conditions in the acidified chambers represented a significant change from conditions likely to be experienced over a full annual cycle in Antarctica[20,23,24,38,39]. During the experimental phase, mean pH in the acidified chambers was 7.688 ± 0.079, the mean saturation state of aragonite was 0.62 ± 0.13 and the mean fCO_2 was 912 ± 150 µatm. These conditions are within the range predicted under the IPCC RCP8.5 "business as usual" scenario by 2100[30]. The antFOCE system, in line with xFOCE goals[14], altered and maintained a pH offset in the acidified chambers that closely tracked the diel variation observed in the control chambers (Fig. 7), when the system was operating normally. System outages, however, resulted in periods of diel variability in the acidified chambers (mean range of 0.24 ± 0.17) that were much larger than the control chambers or ambient conditions (Supplementary Table S2). The pH reverted fully or partially back to ambient during outages (Supplementary Table S1).

High resolution observations of pH are sparse in Antarctic coastal waters, but where available they indicate short term (daily to weekly) variation to be as high as 0.13 over the course of hours and up to 0.27 over several days in McMurdo Sound[23,40]; and up to 0.13 on the Antarctic Peninsula[24]. Thus the increased variability in

acidified chambers is not outside the range of natural fluctuations currently experienced in some coastal Antarctic regions. In a global context the large diel variability in acidified treatments was not as extreme as the short-term pH variability (days to weeks) observed in other coastal ecosystems[22], including kelp forests (range: 0.544), estuaries (range: 0.992), upwelling systems (range: 0.467) and CO_2 vents (range: 1.43).

The large diel variation in pH and other carbonate parameters observed in the acidified treatments will need to be considered when interpreting the biological responses, but these large pH fluctuations may provide insights into the level of resilience of Antarctic benthic communities to rapid changes in environmental conditions. This is especially relevant as future pH variability is expected to increase with reduction in the buffer capacity of seawater as more CO_2 is absorbed from the atmosphere, particularly in polar waters[8,41,42]. Understanding how diel and seasonal variability in dissolved CO_2 parameters will change in response to future ocean acidification is of great interest to the biogeochemistry community and FOCE technology is a useful tool for investigating these changes under *in-situ* conditions of natural variation where multiple drivers of changes in pH occur.

The pH of the control chambers also had greater variability than that measured in the ambient environment. A similar observation was made in the European FOCE experiment (eFOCE)[28] conducted on a seagrass meadow, where the median diel pH variation was 75% greater in the control chambers compared to the ambient environment. The mean diel pH variation in antFOCE control chambers was as much as 285% greater (Fig. 3, Supplementary Table S2). This variation could have been due to the influence of the chambers themselves on the enclosed biological communities, or alternatively, biological activity or gas exchange within the sample lines may have contributed to the observed changes. It is unlikely that other physical processes within the sample lines, such as warming, could be responsible for such variations in pH, as temperature changes caused by the heat trace in the sample lines (~3 °C of warming at the sensors) for example, were accounted for when adjusting measured pH values to *in-situ* conditions. The small volume of air that was occasionally observed in the sample hoses may have contaminated seawater sampled from the chambers, although this volume of air was very small when compared to the volume of water being sampled. Furthermore, a comparison of calculated pH_{tot} from samples of DIC, TA and nutrients simultaneously collected from the surface sampling system and from inside one of the control chambers with a Niskin bottle, agreed to within pH 0.001. This indicates that the carbonate chemistry of the seawater as it was pumped from the chambers to the surface sensor array did not change substantially and suggests that much of the difference between the ambient pH and the pH measured in the antFOCE chambers was caused by greater variability in biological production inside the chambers themselves.

Observations of the seasonal variation in coastal carbonate chemistry in Antarctica are currently limited to four regions[20,23,24,39]. A seasonal cycle of carbonate chemistry in coastal Antarctica features pH values elevated by primary production in summer and lower values during winter driven by net heterotrophy. At McMurdo station in the Ross Sea for example, coastal pH ranges from 7.93 in June to 8.24 in January, with Ω_{ar} in January ranging from 1.79 to 2.03, while in June it reaches 1.03[23]. At Davis Research Station, East Antarctica, carbonate system parameters were measured between May and February, and the seasonal cycle of pH was found to vary from a low of 7.99 in September to 8.20 in January, while Ω_{ar} varied from 1.19 to 1.92 seasonally[20]. Seasonal ranges of pH observed at other Antarctic coastal sites vary from 0.27 at Ryder Bay[43] and 0.53 at Palmer Station[24] on the West Antarctic Peninsula; to 0.42 at McMurdo Sound[23]; to 0.21 at Davis in East Antarctica[20,38].

This seasonal cycle is an important consideration for future FOCE experiments in polar regions, as a pH perturbation performed only in summer may not fully represent the extremes in carbonate chemistry that organisms will be exposed to under future atmospheric CO_2 scenarios. For example, a −0.4 pH offset from ambient conditions maintained over a full year could result in pH levels as low as 7.53 in late winter. This is particularly relevant for Antarctic organisms that have life cycles across multiple seasons such as shelled pteropods[44]; invertebrates with sensitive larval stages[45,46]; or organisms with extremely long developmental periods[47]. Laboratory based ocean acidification experiments have shown adverse effects to the larval stages of Antarctic invertebrates at pH levels of 7.6–7.8[48–50], which suggests that the timing of key life stages in relation to future changes in the seasonal cycle of carbonate chemistry will be important for an organism's likelihood of survival. The weakly calcified shells (non-living) of Antarctic invertebrates have been shown to be vulnerable to dissolution, at a pH of 7.4 and Ω_{ar} of 0.47, within 14–35 days, with exposure of aragonitic or calcitic prisms in the inner shell architecture after 56 days[51]. Antarctic marine fauna have narrow physiological capabilities and are among those with the most limited capacity to cope with environmental change[46], such as a very narrow window of tolerance to changes in temperature[52]. However, their capacity to cope with pH change is relatively poorly understood.

Short-term ambient variability in carbonate chemistry. A comparison of observed ambient pH and dissolved oxygen concentrations at two separate locations within O'Brien Bay demonstrates the spatially variable nature of carbonate chemistry within Antarctic coastal ecosystems. The differences between the two sites are not only observed in the average daily carbonate parameters but are also apparent in the diel variability. The outer site had higher pH and dissolved oxygen concentrations (Figs 3, 4 and 6) and greater diel variability compared to the experiment site, particularly later in the summer (Figs 4 and 5). This variability was most likely driven by the different rates of biological productivity influenced by the different light regimes over each site. Thicker multi-year sea ice over the experiment site would have reduced the amount of light available for photosynthetic communities, compared to the thinner first-year ice over the outer site. The increased light availability at the outer site would have also exposed the area to greater diel variation in light, and therefore greater diel variability in biological productivity, particularly as the near 24-hour daylight at the start of the study period transitioned to day night cycles towards the end of summer. Further changes to light availability, such as variation in snow cover, may have also played a role. Differences in stratification or freshwater input are unlikely to be responsible for differences between sites, as a comparison of temperature and salinity between each site showed no significant differences (Figs 5 and 6) and salinity could explain similar amounts of variation in pH at both sites. This large degree of daily variation has also been observed under similar environmental conditions in McMurdo Sound in the Ross Sea[23,40].

Estimates of primary production indicate it was highly variable, switching from net heterotrophy to net production from day to day. Both carbon- and oxygen-based methods of estimating NCP agreed well with each other, which showed that each site, on average, was net autotrophic during the study period. However, given the large measurement uncertainties of our calculated DIC values, there are limitations in being able to accurately resolve the processes responsible for relatively small changes over short timescales. The calculated average NCP (2 and 3 mmol C m^{-2} day^{-1}) of this study is somewhat less than the values observed in summer (December to February) at other Antarctic coastal sites; for example NCP in Ryder Bay on the West Antarctic Peninsula had an average value of 28 mmol C m^{-2} day[43,53] and NCP in Prydz Bay, East Antarctica[20], had an average value of 17 mmol C m^{-2} day^{-1}. However, the higher sampling frequency of this study showed that daily NCP values could be as high as 131 mmol C m^{-2} day^{-1} and as low as −142 mmol C m^{-2} day^{-1}.

It is apparent that natural variability over small localised spatial scales needs to be better characterised to understand drivers of carbonate chemistry in Antarctic coastal waters to aid in assessment of potential future effects of ocean acidification. Such information will also greatly assist in planning and interpreting manipulative field experiments like FOCE. Monitoring of ambient conditions revealed local variations in pH that were likely to be driven by differences in biological productivity (as measured by dissolved oxygen concentration) and salinity. There was a strong relationship between NCP (as indicated by dissolved oxygen) and pH observed in distanced-based linear models where oxygen could explain between 37 and 47% of the variation in pH. Light plays an important role in determining community composition in polar coastal waters[54,55]. Increases in available light on the seabed via changes in sea ice patterns may also have important influences on variability of pH in Antarctic coastal ecosystems through increased primary production and CO_2 drawdown. Changes in sea ice cover and increasing atmospheric CO_2 concentrations may synergistically affect benthic communities, promoting the growth of macroalgae in habitats under ice currently dominated by invertebrates.

Salinity had an even stronger correlation with pH at both sites, explaining between 53 and 80% of pH variation. This is likely to be due to inputs of freshwater from glacial ice and snow melt, which are also predicted to increase under future climate change scenarios[56]. Understanding drivers of local variability and the natural range of pH that organisms are already subjected to is important in manipulative pH experiments and will improve our understanding of the effects of ocean acidification across a wide variety of marine ecosystems.

In summary, this is the first *in-situ* experiment in a polar region to successfully create predicted ocean acidification conditions using CO_2 enrichment in a controlled way. The FOCE *in-situ* system provides means to address some of the critical gaps in ocean acidification research[16] such as full community representation (including natural, undisturbed microbial communities), under natural conditions of food availability, light and carbonate system parameters, without hydrodynamic isolation. FOCE represents an important complementary method to established techniques using laboratory based experiments, mesocosms or natural analogues such as CO_2 vents[57,58].

Methods

The antFOCE system was deployed in a small sheltered embayment within the larger O'Brien Bay (Fig. 8) in December 2014 after divers had surveyed for suitable areas to locate the experimental setup. The site was selected based on the following criteria: 1) accessibility from shore, 2) shallow water depth (for convenient diver access), 3) a mixed habitat of soft sediment and small boulders that supported a diverse and abundant invertebrate community, and 4) absence of contamination from Casey Research Station. The antFOCE experiment consisted of two replicate acidified chambers (chambers A and B) and two replicate control chambers (chambers C and D), which enclosed sections of seabed; and two open control plots (no chambers, plots E and F), at a depth of ~13 m beneath sea ice. The ice was approximately 260 cm thick at the start of the experiment and 200 cm thick by the end. The pH within the acidified chambers was manipulated by the incremental addition/adjustment of CO_2 enriched seawater (ESW). This was controlled and monitored by a surface sensor array and a series of adjustable pumps and switchable taps (Fig. 9d) that also allowed seawater to be sampled from the surface. The chambers were placed on patches of sediment (Fig. 9a) at least 10 cm deep and at least 9 m^2 in extent so that sediment/water interactions could be monitored. The benthic habitat was a mixture of boulders, cobbles and patches of sediment (Fig. 9a) and was dominated by marine invertebrates, with no macroalgae present due to the multi-year sea ice reducing light availability. The sediment was covered with a layer of microphytobenthos, consisting primarily of diatoms[59]. Divers deployed the underwater components over a period of several weeks while the surface system was transported to the site and assembled. A schematic diagram of the system is shown in Supplementary Fig. S4.

CO_2 Enriched Seawater (ESW). Seawater from near the seabed, close to the experiment site, was pumped to the surface and saturated with CO_2 in a pressurized cylinder (internal measurements 1520 mm long × diameter 240 mm, internal volume 69 L), which contained a roughly equal mix of air and CO_2, held at approximately 1.6 atmospheres in order to ease the load on the dosing pump pushing ESW into the underwater chambers. The ESW system was housed in a shipping container with the generator. A mass flow controller (Alicat M series) was used to measure the amount of CO_2 being used, which was supplied from a bank of 69 CO_2 cylinders (food grade F size cylinder, holding 22 kg of CO_2) stored on site adjacent to the generator van. The ESW cylinder contained a misting showerhead at the top and was filled with plastic bio-balls (OVI-Flow ball 2 Biologic Media) to increase the surface area available for diffusion. The ESW, which had an approximate pH of 5.5 and a CO_2-enrichment factor in excess of 30, was introduced to the seabed experimental setup via a pump and hose system, as discussed below.

The chemical equilibrium of FOCE experiments is dependent on a time delay following addition of ESW, due to the relationship between pH, CO_2 concentration and temperature as defined by the CO_2 kinetic model of e-folding time (τ)[29]. In FOCE experiments, equilibrium between the various carbonate species is assumed to be reached at $3 \times \tau$[14]. Given seawater temperatures of approximately −1.2 °C and a flow rate of ~8 L min^{-1} within the

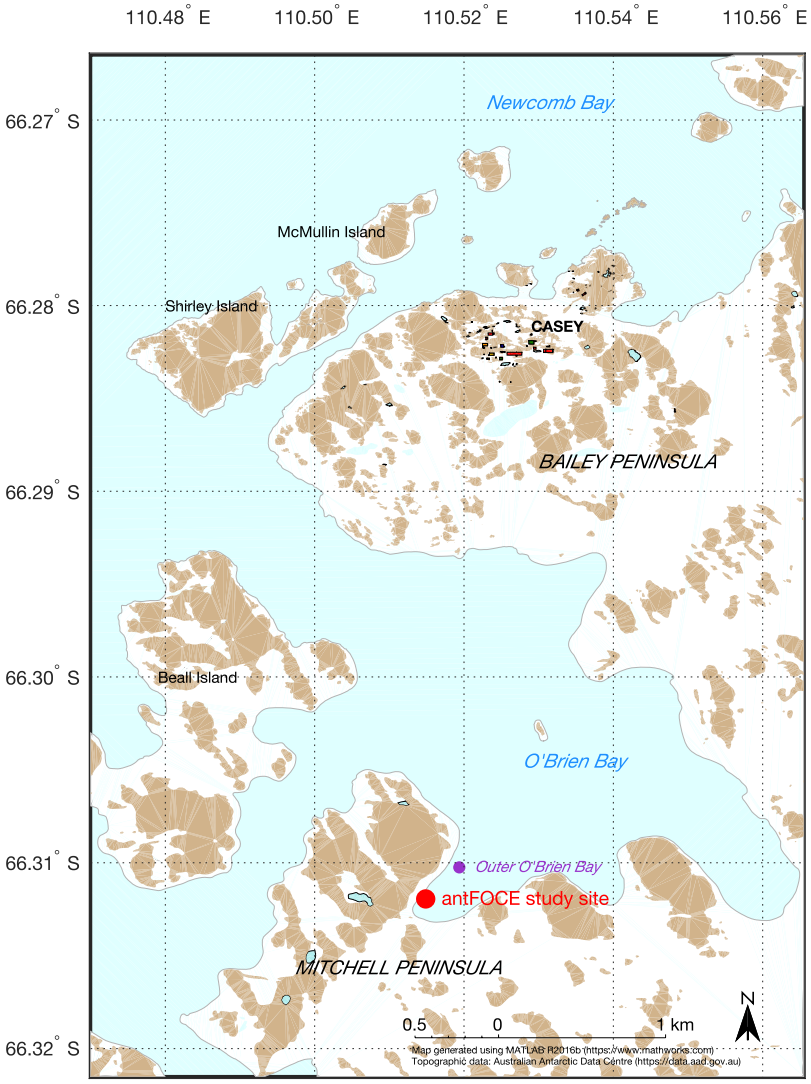

Figure 8. Map showing the location of the antFOCE experiment at Casey Research Station in East Antarctica. The experiment was conducted in a small bay within O'Brien Bay, between the Mitchell and Bailey Peninsulas in the Windmill Islands. Red dot shows location of the antFOCE experiment and location of the SeapHOx unit near the experiment; the purple marker for outer O'Brien Bay shows the location of the second SeapHOx unit. Map made using the mapping toolbox in MATLAB R2016b (https://www.mathworks.com). The topographic data was obtained from the Australian Antarctic Data Centre (https://data.aad.gov.au/aadc/portal/drill_down.cfm?id=14) and used with permission under the Creative Commons Attribution 3.0 Unported License.

equilibration ducting, it was determined that 40 metres of ducting would be required for full chemical equilibration of the ESW to occur before it reached the experimental chambers.

Seabed experimental setup. The four chambers were constructed from clear polycarbonate material (Fig. 9a) that measured 2000 mm length × 500 mm width × 500 mm height, with three hinged lids on the top of the chamber and an open bottom. On the outlet end of the chamber there was a 10 mm stainless steel mesh screen. A 280 mm wide rubber skirt flap was attached to the base of the chamber to help seal the sides (Fig. 9a). The chamber was attached to a 40 m long cylindrical equilibration duct (Plastcorp Mine flex stainless with steel wire; 500 mm diameter) via a stainless steel collar (Fig. 9a,c). Each duct consisted of 4 × 10 m long sections joined with stainless steel collars. The inlet end of the duct was attached to 3.5 m of PVC storm water pipe, known as the thruster tube. Each thruster tube consisted of two sections of PVC pipe (250 mm diameter) joined with a collar. The ESW was introduced to the start of the pipe just behind the open end used for the intake of surrounding seawater, which was fitted with a cylindrical section of 10 mm stainless steel mesh (370 mm long, 250 mm diameter) to prevent the ingress of fish and large invertebrates. In the second section, a thruster (Navigator 65-5501) drew water into the pipe past a flow meter (General Oceanics digital lower flow) and into the duct and then eventually through the chamber. Water flow through the system was unidirectional and maintained at 3 cm s^{-1}, based on measurements taken at the site which showed background currents to range from 1 to 2 cm.s^{-1}. The decision to use a slightly higher velocity was made to minimize the settlement of water borne particulates in the 40 m mixing ducts.

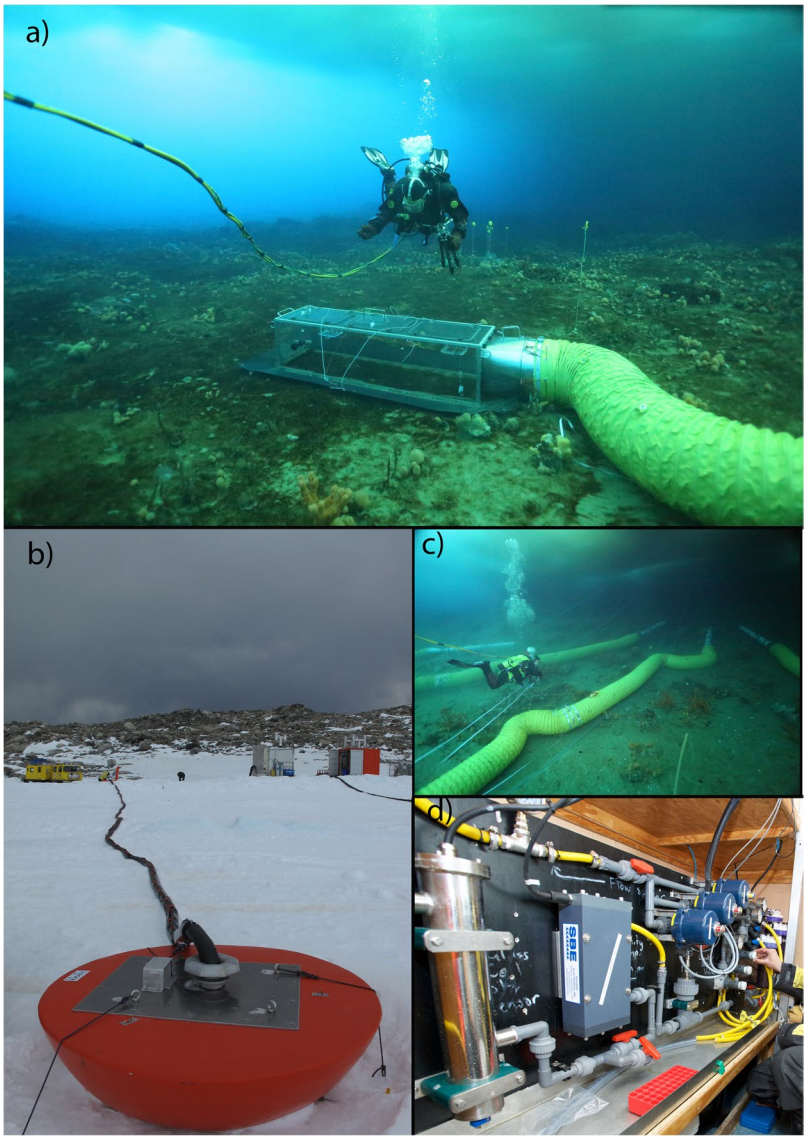

Figure 9. Photographs of the antFOCE system. (**a**) A diver over one of the experimental chambers, which is attached to an equilibration duct (Photo: J. Stark); (**b**) surface equipment at the antFOCE field site, with the sea-ice buoy and insulated umbilical in foreground, and the 'Silver Chalet', containing the surface sensor array, and orange container housing the generator and CO_2 ESW system visible in the background (Photo: J. Stark); (**c**) the equilibration ducting with white thruster tubes attached (Photo: J. Stark); (**d**) the surface sensor array inside the Silver Chalet (Photo: N. Roden).

Pump system and hoses. Peristaltic pumps were used to: 1) pump ambient seawater from near the chambers to the ESW unit (1× Albin peristaltic ALP17 56 RPM fixed), 2) pump ESW down to the thruster tubes (2× Albin peristaltic ALP17 29-6 RPM variable output speed), and 3) pump water from the chambers to the sensor panel (3× Albin peristaltic ALP17 29 RPM fixed). These pumps were contained in a large insulated plastic box (Techni Ice 1100 L), which was heated internally with a diesel-burning heater (Webasto WEB902023480B). Pressure rated hoses were used to draw up water to use in the manufacture of ESW (PVC Plutone clear/wire suction internal diameter 19 mm) and to the sensor panel from the chambers (PVC Plutone clear/wire suction 16 mm), as well as carry ESW to the thruster tubes (Barfell Diver air, internal diameter 10 mm). The hoses were wrapped in a double coil of heat trace and all wrapped by a layer of insulation (FR Armaflex) contained within a canvas wrapping, to prevent seawater freezing in the sub-zero air temperatures (Fig. 9b). The umbilical of the hoses, which also contained a 240 V power cable, crossed the surface of the sea ice to a large metal sea-ice buoy, which sat in a 0.9 m diameter hole in the sea ice (Fig. 9b). The umbilical and cables passed through the centre of the buoy, into the water (Fig. 9b), and out to the seabed experimental setup. Power to the entire antFOCE system was supplied from a Cummins C22 D5 (X series) generator, housed on-site in a shipping container. An adjacent 400 L tank of diesel fuel was connected to the generator and regularly refilled from 200 L drums transported to the site.

Sensor array. Water was continuously pumped from the outlet end of three of the benthic chambers (both acidified chambers and one control, manually alternating between chamber C and D) to the surface where it was pumped through the sensor array, which was housed in an insulated building mounted on a sled, known as the Silver Chalet, which also housed the computers and electronic control equipment (Fig. 9b and d). To obtain measurements, valves were used to enable water to flow sequentially from each chamber over the sensors for 10 minute periods. Water from chambers not being passed over the sensors went into an overflow disposal line. The sensor array consisted of a dissolved oxygen optode (Aanderaa, model 3835), thermosalinograph (Seabird SBE 45 MicroTSG), and for redundancy, two pH electrodes (Seabird SBE 18 and Honeywell Durafet). Water from the chambers was sampled for biogeochemical measurements using a valve on the water line leading into the sensor array. An additional pH electrode (Seabird SBE 18) was moved between chambers as a means to compare pH measurements *in-situ* with those from the surface sensor panel.

Control of pH. The pH of the acidified chambers was controlled by varying the amount of ESW pumped into the thruster tubes/equilibration ducts to achieve the −0.4 pH offset. The pH was measured by the Honeywell Durafet sensor and the flow rate of the ESW was adjusted slowly by a feedback control loop to ensure stability. Due to the surface sensor system cycling through each chamber every 10 minutes, and the seawater itself taking ~10 minutes to be pumped from the chamber to the surface, a delay of 30 minutes between estimates of pH offset was introduced. Adjustments to pH in the acidified chambers would then take another 10 minutes to propagate back down the ESW line and a further 22 minutes to flow through the equilibration ducting and into the chambers, introducing a total delay of ~1 hour in adjusting the pH within a chamber. This is necessary to let the CO_2 chemistry reach equilibrium and create a true pH-altered environment as opposed to a high CO_2 partial pressure situation[29].

Biogeochemical measurements. Discrete seawater samples of 250 mL, used for the analysis of DIC and TA, were collected from the surface sampling system and from a Niskin bottle at various locations within the study site. A preservative of 100 µL of a saturated $HgCl_2$ solution was added to these samples to halt biological activity. DIC was determined using a Single Operator Multiparameter Metabolic Analyser (SOP 2)[60], and TA was determined by open-cell potentiometric titration using a 0.1 M hydrochloric acid titrant (SOP 3b)[60]. Routine analysis of Certified Reference Material (batch 137) from Scripps Institution of Oceanography were used to verify the measurement accuracy and precision for DIC and TA analyses, which were better than ±1.0 µmol kg^{-1} and ±1.3 µmol kg^{-1} respectively. Dissolved nutrient concentrations for nitrate, nitrite, phosphate and silicic acid were determined using standard colorimetric methods[61], adapted for flow injection analysis on a SEAL AutoAnalyzer 3 HR, and yielded a measurement precision of ±0.4 µmol kg^{-1}, ±0.01 µmol kg^{-1}, ±0.06 µmol kg^{-1} and 3 µmol kg^{-1}, respectively.

The pH electrodes in the antFOCE system were calibrated using calculated pH_{tot} values (accuracy and precision pH ±0.005, based on propagated uncertainties of measured parameters), that were determined approximately every three days using measurements of total dissolved inorganic carbon (DIC), total alkalinity (TA) and nutrients from the discrete bottle seawater samples. Calculations were made using the standard set of carbonate system equations with the CO2SYS program[62] and the dissociation constants of Roy, *et al.*[63]. Due to minimal drift in the Honeywell Durafet sensor with a stability better than pH ±0.005 over weeks to months[64], a mean offset correction was applied based on all calibration samples. Significant sensor drift occurred in the Seabird SBE 18 electrodes, which required an alternative calibration procedure, whereby it was assumed that the sensor drift was linearly proportional in time. However, this procedure did not significantly improve the data quality. It was determined that the drift was variable in nature and not readily corrected. As such, only the Honeywell Durafet data are considered here.

Two SeapHOx units[64,65] were deployed on the seafloor in O'Brien Bay to measure ambient pH, dissolved oxygen, temperature and salinity at 1 hour intervals from 16 December 2014 to 28 February 2015. The units were located in 13 m of water: one adjacent to the thruster tubes of the antFOCE system (experiment site) and used to characterize the ambient seawater conditions, and the other ~300 m further towards the mouth of O'Brien Bay (outer O'Brien Bay; Fig. 8) to asses variability within the bay. Honeywell Durafet pH sensors inside the SeapHOx units were calibrated using the approach described previously, by collecting samples next to the SeapHOx units with a Niskin bottle. Oxygen optodes (Aanderaa, model 3835) were calibrated at the Commonwealth Scientific and Industrial Research Organisation (CSIRO) Ocean Carbon Laboratory in Hobart, Tasmania, Australia before and after deployments using Winkler titrations. The calibration data were used to fit the optode response to a Stern-Volmer equation[66], and yielded a relative accuracy of ±2 µmol kg^{-1}. Data from the oxygen optode in the surface sensor array were affected by air bubbles trapped inside its housing and are not considered any further in this study. The oxygen concentration at saturation was determined from atmospheric pressure, seawater temperature and salinity measurements[67]. Temperature and salinity were measured using two SBE 37-SI MicroCAT conductivity and temperature recorders that were calibrated at the CSIRO Oceanographic Calibration Facility in Hobart, Tasmania, Australia, and yielded an accuracy of ±0.002 °C and ±0.004, respectively.

TA data from this study were combined with data from previous studies in the Southern Ocean that used the same measurement techniques, and a linear regression of salinity versus TA was calculated. This relationship (Fig. 2) was used to calculate TA from high-resolution salinity measurements. Data used to calculate the regression were from samples shallower than 500 m and south of 60°S and included measurements from the CO_2/World Ocean Circulation Experiment (WOCE) hydrographic sections of the nearby Princess Elizabeth Trough in 2005, measurements from the southern end of the 1994 WOCE SR3 transect along 140°E, and measurements from the Baseline Research on Oceanography, Krill and the Environment – West (BROKE-West) study in 2006[68]. The correlation between the parameters in Fig. 2 ($y = (62.8 \pm 0.4)x + (163 \pm 13)$; $n = 340$, $r^2 = 0.99$, standard error = 4 µmol kg^{-1}) indicates net calcification/dissolution of carbonate minerals in the water column was not

a significant contributor to the TA variability. The saturation state of aragonite (Ω_{ar})[69] and the fugacity of CO_2 (fCO_2) were calculated from high-resolution measurements of pH_{tot}, calculated TA, and the mean phosphate and silicic acid concentrations measured throughout the experimental period of $1.8 \pm 0.2\,\mu mol\,kg^{-1}$ and $50 \pm 9\,\mu mol\,kg^{-1}$, respectively. Propagating the uncertainties associated with these measured and calculated input parameters, we estimate an uncertainty of ± 0.01 for Ωar and $\pm 8\,\mu atm$ for $fCO2$. All carbonate chemistry data is available at https://doi.org/10.4225/15/5a28b5eb04f71.

The NCP estimates for each SeapHOx deployment were calculated using a mass balance approach by averaging the calculated DIC concentrations for each day and subtracting one day's value from the previous to estimate at a total daily DIC change. This change is considered to be the sum of changes due to freshwater flux from ice formation/melt, biology and air-sea flux, and was calculated using established procedures[20]. The biological component of this change can therefore represent the net community production (where positive) or net community respiration (where negative) for an entire 24 hour period. Oxygen-based "Redfield" estimates of NCP were calculated by dividing the daily change in oxygen by 1.4 to allow expression in terms of organic carbon production, or DIC uptake[33].

Data analysis. A four factor permutational analysis of variance (PERMANOVA[70,71]) was used to examine the differences in pH at five time scales, with the factors Month (3 levels), Week (3 to 5 levels, nested in month), Day (7 levels, nested in week), Diel (AM/PM, nested in day) and Hour (replicate measurements, residual variation). The analysis was based on the Euclidean distance similarity matrix with Type III (partial) sums-of-squares calculated using 999 unrestricted permutations of the raw data. PERMANOVA was also used to estimate the components of variation, a measure of the magnitude of effect size, for each temporal scale. Distance-based linear modelling of the relationship between pH and salinity, temperature and oxygen concentration were explored using the DISTLM procedure[35,71], based on a Euclidean distance similarity matrix for pH and normalised salinity, temperature and dissolved oxygen.

References

1. IPCC. *Climate Change 2014: Synthesis Report. Contribution of Working Groups I, II and III to the Fifth Assessment Report of the Intergovernmental Panel on Climate Change*. (IPCC, 2014).
2. Sanford, T., Frumhoff, P. C., Luers, A. & Gulledge, J. The climate policy narrative for a dangerously warming world. *Nature Climate Change* **4**, 164–166 (2014).
3. Peters, G. P. *et al*. The challenge to keep global warming below 2°C. *Nature Climate Change* **3**, 4–6 (2013).
4. Le Quéré, C. *et al*. Global Carbon Budget 2016. *Earth Syst. Sci. Data* **8**, 605–649, https://doi.org/10.5194/essd-8-605-2016 (2016).
5. Orr, J. C. *et al*. Anthropogenic ocean acidification over the twenty-first century and its impact on calcifying organisms. *Nature* **437**, 681–686 (2005).
6. Pörtner, H.-O. *et al*. In *Climate Change 2014: Impacts, Adaptation, and Vulnerability. Part A: Global and Sectoral Aspects. Contribution of Working Group II to the Fifth Assessment Report of the Intergovernmental Panel on Climate* Change (eds C.B. Field, V.R. Barros, D.J. Dokken, K.J. Mach, M.D. Mastrandrea, T.E. Bilir, K.L. Ebi M. Chatterjee, Y.O. Estrada, R.C. Genova, B. Girma, E.S. Kissel, A.N. Levy, S. MacCracken, P.R. Mastrandrea, & L.L. White) 411–484 (2014).
7. Kroeker, K. J. *et al*. Impacts of ocean acidification on marine organisms: quantifying sensitivities and interaction with warming. *Glob Change Biol* **19**, 1884–1896, https://doi.org/10.1111/gcb.12179 (2013).
8. Fabry, V. J., McClintock, J. B., Mathis, J. T. & Grebmeier, J. M. Ocean Acidification at High Latitudes: The Bellwether. *Oceanography* **22**, 160–171 (2009).
9. Doney, S. C. *et al*. Climate Change Impacts on Marine Ecosystems. *Annual Review of Marine Science* **4**, https://doi.org/10.1146/annurev-marine-041911-111611 (2012).
10. McNeil, B. I. & Matear, R. J. Southern Ocean acidification: A tipping point at 450-ppm atmospheric CO_2. *PNAS* **105**, 18860–18864 (2008).
11. Steinacher, M., Joos, F., Frölicher, T. L., Plattner, G. K. & Doney, S. C. Imminent ocean acidification in the Arctic projected with the NCAR global coupled carbon cycle-climate model. *Biogeosciences* **6**, 515–533, https://doi.org/10.5194/bg-6-515-2009 (2009).
12. Bednaršek, N. *et al*. Extensive dissolution of live pteropods in the Southern Ocean. *Nature Geosci* **5**, 881–885, https://doi.org/10.1038/ngeo1635 (2012).
13. Hofmann, G. E. *et al*. The Effect of Ocean Acidification on Calcifying Organisms in Marine Ecosystems: An Organism-to-Ecosystem Perspective. *Annual Review of Ecology, Evolution, and Systematics* **41**, 127–147 (2010).
14. Gattuso, J. P. *et al*. Free Ocean CO_2 Enrichment (FOCE) systems: present status and future developments. *Biogeosciences* **11**, 4057–4075, https://doi.org/10.5194/bgd-11-4001-2014 (2014).
15. Kerrison, P., Hall-Spencer, J. M., Suggett, D. J., Hepburn, L. J. & Steinke, M. Assessment of pH variability at a coastal CO_2 vent for ocean acidification studies. *Estuarine, Coastal and Shelf Science* **94**, 129–137 (2011).
16. Riebesell, U. & Gattuso, J.-P. Lessons learned from ocean acidification research. *Nature Climate Change* **5**, 12–14 (2015).
17. Queirós, A. M. *et al*. Scaling up experimental ocean acidification and warming research: from individuals to the ecosystem. *Glob Change Biol* **21**, 130–143 (2015).
18. Matson, P. G., Washburn, L., Martz, T. R. & Hofmann, G. E. Abiotic versus biotic drivers of ocean pH variation under fast sea ice in McMurdo Sound, Antarctica. *PLoS ONE* **9**, e107239 (2014).
19. Waldbusser, G. G. & Salisbury, J. E. Ocean Acidification in the Coastal Zone from an Organism's Perspective: Multiple System Parameters, Frequency Domains, and Habitats. *Annual Review of Marine Science* **6**, 221–247, https://doi.org/10.1146/annurev-marine-121211-172238 (2014).
20. Roden, N. P., Shadwick, E. H., Tilbrook, B. & Trull, T. W. Annual cycle of carbonate chemistry and decadal change in coastal Prydz Bay, East Antarctica. *Marine Chemistry* **155**, 135–147 (2013).
21. Smith, W. O., Dinniman, M. S., Hofmann, E. E. & Klinck, J. M. The effects of changing winds and temperatures on the oceanography of the Ross Sea in the 21st century. *Geophysical Research Letters* **41**, 1624–1631 (2014).
22. Hofmann, G. E. *et al*. High-Frequency Dynamics of Ocean pH: A Multi-Ecosystem Comparison. *PLoS ONE* **6**, e28983, https://doi.org/10.1371/journal.pone.0028983 (2011).
23. Kapsenberg, L., Kelley, A. L., Shaw, E. C., Martz, T. R. & Hofmann, G. E. Near-shore Antarctic pH variability has implications for the design of ocean acidification experiments. *Sci. Rep*. **5** (2015).
24. Schram, J. B., Schoenrock, K. M., McClintock, J. B., Amsler, C. D. & Angus, R. A. Multi-frequency observations of seawater carbonate chemistry on the central coast of the western Antarctic Peninsula. *Polar Research* **34** (2015).
25. Walz, P., Kirkwood, W., Peltzer, E., Hester, K. & Brewer, P. In *OCEANS 2008-MTS/IEEE Kobe Techno-Ocean*. 1–4 (IEEE).
26. Kirkwood, W. *et al*. In Underwater Technology (UT), 2011 IEEE Symposium on and 2011 Workshop on Scientific Use of Submarine Cables and Related Technologies (SSC). 1–8 (IEEE).

27. Kline, D. I. *et al*. A short-term *in situ* CO_2 enrichment experiment on Heron Island (GBR). *Sci. Rep.* **2**, 413–411 (2012).
28. Cox, T. E. *et al*. Effects of *in situ* CO_2 enrichment on structural characteristics, photosynthesis, and growth of the Mediterranean seagrass *Posidonia oceanica*. *Biogeosciences* **13**, 2179–2194, https://doi.org/10.5194/bg-13-2179-2016 (2016).
29. Zeebe, R. & Wolf-Gladrow, D. CO_2 in Seawater: Equilibrium, Kinetics, Isotopes. In *Elsevier Oceanography Book Series, 65* 346 (Elsevier Amsterdam 2005).
30. IPCC. *Climate Change 2013: The Physical Science Basis. Contribution of Working Group I to the Fifth Assessment Report of the Intergovernmental Panel on Climate Change*. (2013).
31. Brewer, P. G. & Goldman, J. C. Alkalinity changes generated by phytoplankton growth. *Limnol. Oceanogr* **21**, 108–117 (1976).
32. Archer, D., Emerson, S. & Reimers, C. Dissolution of calcite in deep-sea sediments: pH and O_2 microelectrode results. *Geochimica et Cosmochimica Acta* **53**, 2831–2845 (1989).
33. Laws, E. A. Photosynthetic quotients, new production and net community production in the open ocean. *Deep Sea Research Part A. Oceanographic Research Papers* **38**, 143–167 (1991).
34. Bender, M., Orchardo, J., Dickson, M.-L., Barber, R. & Lindley, S. *In vitro* O_2 fluxes compared with ^{14}C production and other rate terms during the JGOFS Equatorial Pacific experiment. *Deep Sea Research Part I: Oceanographic Research Papers* **46**, 637–654 (1999).
35. Legendre, P. & Anderson, M. J. Distance-based redundancy analysis: Testing multispecies responses in multifactorial ecological experiments. *Ecological Monographs* **69**, 1–24 (1999).
36. Anderson, M. J. & Robinson, J. Permutation tests for linear models. *Australian & New Zealand Journal of Statistics* **43**, 75–88 (2001).
37. McLeod, A. & Long, S. Free-air carbon dioxide enrichment (FACE) in global change research: a review. *Advances in ecological research* **28**, 1–56 (1999).
38. Gibson, J. A. E. & Trull, T. W. Annual cycle of fCO_2 under sea-ice and in open water in Prydz Bay, East Antarctica. *Marine Chemistry* **66**, 187–200, https://doi.org/10.1016/s0304-4203(99)00040-7 (1999).
39. Legge, O. J. *et al*. The seasonal cycle of ocean-atmosphere CO_2 flux in Ryder Bay, west Antarctic Peninsula. *Geophysical Research Letters* **42**, 2934–2942 (2015).
40. Matson, P. G., Martz, T. R. & Hofmann, G. E. High-frequency observations of pH under Antarctic sea ice in the southern Ross Sea. *Antarctic Science* **23**, 607–613 (2011).
41. Shadwick, E., Trull, T., Thomas, H. & Gibson, J. Vulnerability of polar oceans to anthropogenic acidification: comparison of arctic and antarctic seasonal cycles. *Sci. Rep.* **3**, 2339–2339 (2013).
42. Egleston, E. S., Sabine, C. L. & Morel, F. M. Revelle revisited: Buffer factors that quantify the response of ocean chemistry to changes in DIC and alkalinity. *Global Biogeochemical Cycles* **24** (2010).
43. Jones, E. M. *et al*. Ocean acidification and calcium carbonate saturation states in the coastal zone of the West Antarctic Peninsula. *Deep Sea Research Part II: Topical Studies in Oceanography* **139**, 181–194 (2017).
44. Bednaršek, N., Tarling, G., Fielding, S. & Bakker, D. Population dynamics and biogeochemical significance of Limacina helicina antarctica in the Scotia Sea (Southern Ocean). *Deep Sea Research Part II: Topical Studies in Oceanography* **59**, 105–116 (2012).
45. Peck, L. S., Webb, K. E. & Bailey, D. M. Extreme sensitivity of biological function to temperature in Antarctic marine species. *Functional Ecology* **18**, 625–630 (2004).
46. Peck, L. S. Prospects for surviving climate change in Antarctic aquatic species. *Frontiers in Zoology* **2**, 8 (2005).
47. Peck, L. S., Powell, D. K. & Tyler, P. A. Very slow development in two Antarctic bivalve molluscs, the infaunal clam *Laternula elliptica* and the scallop *Adamussium colbecki*. *Mar Biol* **150**, 1191–1197 (2007).
48. Byrne, M. *et al*. Vulnerability of the calcifying larval stage of the Antarctic sea urchin *Sterechinus neumayeri* to near-future ocean acidification and warming. *Glob Change Biol* **19**, 2264–2275, https://doi.org/10.1111/gcb.12190 (2013).
49. Gonzalez-Bernat, M. J., Lamare, M. & Barker, M. Effects of reduced seawater pH on fertilisation, embryogenesis and larval development in the Antarctic seastar *Odontaster validus*. *Polar Biol* **36**, 235–247, https://doi.org/10.1007/s00300-012-1255-7 (2013).
50. Yu, P. C. *et al*. Growth attenuation with developmental schedule progression in embryos and early larvae of *Sterechinus neumayeri* raised under elevated CO_2. *PLoS ONE* **8**, e52448 (2013).
51. McClintock, J. B. *et al*. Rapid dissolution of shells of weakly calcified Antarctic benthic macroorganisms indicates high vulnerability to ocean acidification. *Antarctic Science* **21**, 449–456 (2009).
52. Peck, L. S. Prospects for survival in the Southern Ocean: vulnerability of benthic species to temperature change. *Antarctic Science* **17**, 497–507 (2005).
53. Legge, O. J. *et al*. The seasonal cycle of carbonate system processes in Ryder Bay, West Antarctic Peninsula. *Deep Sea Research Part II: Topical Studies in Oceanography* **139**, 167–180 (2017).
54. Clark, G. F., Raymond, B., Riddle, M. J., Stark, J. S. & Johnston, E. L. Vulnerability of shallow Antarctic invertebrate-dominated ecosystems. *Aust. Ecol.* **40**, 482–491, https://doi.org/10.1111/aec.12237 (2015).
55. Clark, G. F. *et al*. Light-driven tipping points in polar ecosystems. *Glob Change Biol* **19**, 3749–3761 (2013).
56. Dierssen, H. M., Smith, R. C. & Vernet, M. Glacial meltwater dynamics in coastal waters west of the Antarctic peninsula. *PNAS* **99**, 1790–1795 (2002).
57. Hall-Spencer, J. M. *et al*. Volcanic carbon dioxide vents show ecosystem effects of ocean acidification. *Nature* **454**, 96–99 (2008).
58. Basso, L., Hendriks, I. E., Rodríguez-Navarro, A. B., Gambi, M. C. & Duarte, C. M. Extreme pH conditions at a natural CO_2 vent system (Italy) affect growth, and survival of juvenile pen shells (*Pinna nobilis*). *Estuaries and Coasts* **38**, 1986–1999 (2015).
59. Thompson, B. A. W., Goldsworthy, P. M., Riddle, M. J., Snape, I. & Stark, J. S. Contamination effects by a conventional and a biodegradable lubricant oil on infaunal recruitment to Antarctic sediments: A field experiment. *Journal of Experimental Marine Biology and Ecology* **340**, 213–226 (2007).
60. Dickson, A. G., Sabine, C. L. & Christian, J. R. Guide to best practices for ocean CO_2 measurements. In *PICES Special Publication* Vol. 3 191 (2007).
61. Hansen, H. & Koroleff, F. Determination of nutrients. In *Methods of Seawater Analysis*, Third *Edition* (eds K. Grasshoff, K. Kremling, & M. Ehrhardt) 159–228 (Wiley-VCH Verlag GmbH, 2007).
62. Van Heuven, S., Pierrot, D., Lewis, E. & Wallace, D. MATLAB program developed for CO_2 system calculations. *ORNL/CDIAC-105b. Carbon Dioxide Information Analysis Center, Oak Ridge National Laboratory, US Department of Energy, Oak Ridge, Tennessee* **530** (2011).
63. Roy, R. N. *et al*. The dissociation constants of carbonic acid in seawater at salinities 5 to 45 and temperatures 0 to 45°C. *Marine Chemistry* **44**, 249–267 (1993).
64. Martz, T. R., Connery, J. G. & Johnson, K. S. Testing the Honeywell Durafet® for seawater pH applications. *Limnol. Oceanogr. Methods* **8**, 172–184 (2010).
65. Bresnahan, P. J., Martz, T. R., Takeshita, Y., Johnson, K. S. & LaShomb, M. Best practices for autonomous measurement of seawater pH with the Honeywell Durafet. *Methods in Oceanography* **9**, 44–60 (2014).
66. Uchida, H., Kawano, T., Kaneko, I. & Fukasawa, M. *In situ* calibration of optode-based oxygen sensors. *Journal of Atmospheric and Oceanic Technology* **25**, 2271–2281 (2008).
67. Garcia, H. E. & Gordon, L. I. Oxygen solubility in seawater: Better fitting equations. *Limnol. Oceanogr.* **37**, 1307–1312 (1992).
68. Roden, N. P., Tilbrook, B., Trull, T. W., Virtue, P. & Williams, G. D. Carbon cycling dynamics in the seasonal sea-ice zone of East Antarctica. *Journal of Geophysical Research: Oceans* **121** (2016).

69. Mucci, A. The solubility of calcite and aragonite in seawater at various salinities, temperatures, and one atmosphere total pressure. *American Journal of Science* **283**, 780–799 (1983).
70. Anderson, M. J. A new method of non-parametric multivariate analysis of variance. *Aust. Ecol.* **26**, 32–46 (2001).
71. Anderson, M. J., Gorley, R. N. & Clarke, K. R. *PERMANOVA+ for PRIMER: Guide to software and statistical methods*. (PRIMER-E, 2008).

Acknowledgements

The antFOCE project was funded by the Australian Research Council - Antarctic Gateway Partnership, the Australian Antarctic Division (AAS 4127), an Australian Research Council Linkage Infrastructure, Equipment and Facilities grant (LE130100220) and supported by the University of Tasmania Institute for Marine and Antarctic Studies, CSIRO Oceans and Atmosphere, the Monterey Bay Aquarium Research Institute (USA) and Plymouth Marine Laboratory (UK). NR was supported by an Australian Postgraduate Award and a CSIRO Oceans and Atmosphere scholarship. The authors would like to thank the many people who contributed to the development and deployment of the antFOCE system, in particular Jono Reeve, Matthew Wright, Helena Baird, Cathryn Wynn-Edwards, Martin Riddle, Ian Snape, Lizzy Elliot, Andrew Cawthorn, Clint Berry, Mike Sparg, Kate Stanford, John Runcie, Glenn Dunshea, Tony Press, Nick Gales, David Lyons and the personnel at Casey Research Station for their logistical support throughout the field season. Permits from the Department of the Environment, Australian Government, were provided to conduct this research.

Author Contributions

J.S. and D.R. conceived and designed the experiment, J.S., D.R., G.J., S.W., M.M. and S.S. planned and managed the logistics; N.R. and J.S. wrote the main manuscript text and prepared the figures; N.R., S.S. and K.B. managed the carbonate chemistry laboratory measurements and analysis; J.S., N.R., J.B., G.J., W.K., M.M., E.O., K.B., and S.W. participated in field work; W.K., M.M., K.N., E.P., S.W. and J.S. designed, tested, built and/or ran the experimental system; E.O., B.T., K.B., N.R. and J.S. managed the SeapHOx deployment and data processing; J.S. performed the statistical analysis. All authors reviewed the manuscript.

Additional Information

Supplementary information accompanies this paper at https://doi.org/10.1038/s41598-018-21029-1.

Competing Interests: The authors declare no competing interests.

Publisher's note: Springer Nature remains neutral with regard to jurisdictional claims in published maps and institutional affiliations.

Open Access This article is licensed under a Creative Commons Attribution 4.0 International License, which permits use, sharing, adaptation, distribution and reproduction in any medium or format, as long as you give appropriate credit to the original author(s) and the source, provide a link to the Creative Commons license, and indicate if changes were made. The images or other third party material in this article are included in the article's Creative Commons license, unless indicated otherwise in a credit line to the material. If material is not included in the article's Creative Commons license and your intended use is not permitted by statutory regulation or exceeds the permitted use, you will need to obtain permission directly from the copyright holder. To view a copy of this license, visit http://creativecommons.org/licenses/by/4.0/.

© The Author(s) 2018